EFFECTS OF MORE EXTREME RAINFALL DISTRIBUTION ON VEGETATION PODUCTIVITY IN KENYA
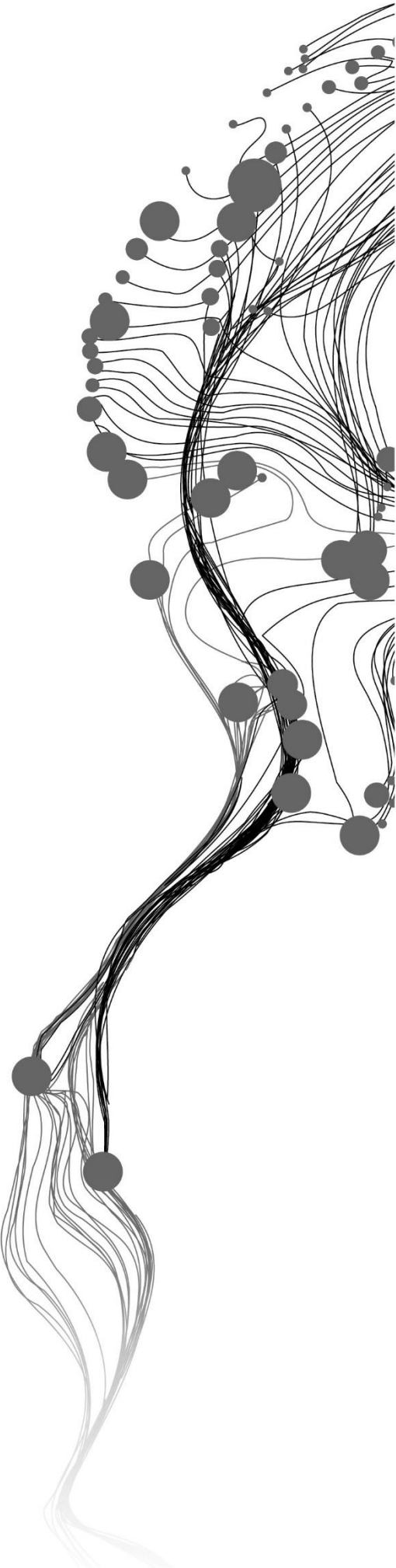
MONICA SIXTUS MNAMBA
February, 2018

SUPERVISORS:
Dr. A. Vrieling
Dr. T.A Groen

EFFECTS OF MORE EXTREME RAINFALL DISTRIBUTION ON VEGETATION PODUCTIVITY IN KENYA

MONICA SIXTUS MNAMBA
Enschede, The Netherlands, February, 2018

Thesis submitted to the Faculty of Geo-Information Science and Earth Observation of the University of Twente in partial fulfilment of the requirements for the degree of Master of Science in Geo-information Science and Earth Observation.
Specialization: Natural Resources Management

SUPERVISORS:
Dr. A. Vrieling
Dr. T.A Groen

THESIS ASSESSMENT BOARD:
Dr. A.D Nelson (Chair)
Dr. F. Fava (External Examiner, International Livestock Research Institute)

ABSTRACT

Climate change is expected to increase the intensity and frequency of extreme weather events. This may result in heavier precipitation events and longer dry periods. Yet the impact of more extreme precipitation distribution on vegetation productivity remains largely unknown, while their consequences on livelihoods that depend on agriculture and livestock keeping can be large. To better understand how more extreme precipitation distribution affects vegetation, this study investigated if and where seasonal extreme precipitation indices can improve the explanation of seasonal vegetation productivity as compared to seasonal rainfall. For this purpose, this study extracted a proxy measure for seasonal above-ground net primary productivity (ANPP) from satellite-derived time series from the 250m resolution Enhanced Moderate Resolution Imaging Spectroradiometer (eMODIS) product. This was achieved by temporally accumulating NDVI between location-specific start- and end-of-season, which were derived from an existing phenological analysis. ANPP time series were compared against *in situ* daily precipitation records of 2001 to 2016 from 19 rainfall stations across Kenya. For most stations, two main rainfall seasons per year were identified. The long-term daily rainfall was then averaged per each station to estimate the start- and end-of-season. Regression analysis showed that seasonal rainfall can explain less than 50% of the ANPP variability. In this study, extreme precipitation indices were calculated per season from daily rainfall records as a way to summarize intra-seasonal rainfall distribution differences between years. It has been observed that the indices can explain an important part of the variability but differs per season and location. Across all the stations, the regression analysis showed that R95pTOT index (precipitation due to wet days-daily rainfall >95th percentile) explain much of variability with an average of R^2 0.63 during the long rains and R^2 0.55 for short rains. The results indicate that extreme precipitation indices can improve in explaining the variability that was not explained by total seasonal rainfall. The study results reveal that more extreme distributions of precipitation have a significant effect on vegetation production and thus need to be considered for predicting climate change impacts on seasonal vegetation productivity.

ACKNOWLEDGEMENTS

TABLE OF CONTENTS

LIST OF FIGURES

LIST OF TABLES

LIST OF ABBREVIATIONS

ANPP	Above-ground Net Primary Productivity
CETRAD	Centre for Training and Integrated Research in Arid and Semi-Arid Lands Development
CumNDVI	Cumulative Normalized Difference Vegetation Index
CumP	Cumulative Precipitation
CDD	Consecutive dry days
eMODIS	Enhanced Moderate Resolution Imaging Spectroradiometer
ETCCDI	Expert Team on Climate Change Detection and Indices
EOS	End of season
ILRI	International Livestock Research Institute
JKIA	Jomo Kenyatta International Airport
JRC	Joint Research Centre of the European Commission
KMD	Kenya Meteorological Department
NDVI	Normalized Difference Vegetation Index
RFE	Rainfall Estimates
R95pTOT	Precipitation due to wet days (daily rainfall >95th percentile)
R95p	Precipitation fraction of total precipitation due to days with rainfall amount >95th percentile
SDII	Simple daily intensity index
SI	Seasonality Index
SOS	Start of season
USGS	United States Geological Survey

1. INTRODUCTION

1.1. Background and problem statement

Climatic changes induced by global warming cause variations in the intensity or frequency of temperature and rainfall extremes, with rainfall increasing during the cold periods and decreasing in the warm periods (Allan and Soden 2008; IPCC 2014). This so-called hydrological cycle amplification (Easterling et al., 2000) results in the increased occurrence of droughts and intense precipitation (Huntington, 2006). This in turn can cause consequences to primary productivity (Kang et al., 2009) because there is less water available during the growing season.

Extreme weather changes over East Africa such as droughts and floods were observed to occur more frequently within the last 30 years to 60 years due to the continued warming of the Indian Ocean (IPCC 2014). "During the last 30 years, the Horn of Africa experienced a persistent decrease in rainfall during the long rains season" (Tierney et al., 2015). Based on current climate models, a further increase in extreme weather is expected for East Africa. A reduction of average annual rainfall and rising temperatures are expected, which will expose agriculture to increased drought stress (Kimani et al., 2014). This in turn may have severe consequences for local food security which largely depends on agriculture and livestock production (Tierney et al., 2015). "Global circulation models predict that by 2100, Kenya's average temperature will increase by 4°C, resulting in higher variability of rainfall and the exceeding magnitude of future hazards" (Muchemi et al., 2012).

Kenya's crop and livestock production are affected by droughts, leading to high malnutrition rates among the vulnerable populations (Kabubo-Mariara & Kabara, 2015). Moreover, these hazards have slowed down the country's economic development (Kimani et al., 2014). Between 1997 to 1998, the reduced rainfall due to an El Niño event resulted in the loss of crops and livestock for a large part of the country (Cumiskey & Jackson, 2016). In 2009, drought caused Kenyan pastoralists to lost more than 50% of livestock (Kimani et al., 2014). From 2016 to the beginning of 2017 the country also experienced drought conditions which caused by the low rainfall and high temperatures. This condition lead over 3 million people in need of food aid (Uhe et al., 2017). On the other hand, from April to May 2013, intense rainstorms in areas located from a distance downstream of Kenya resulted in flash floods, causing displacement for 140,000 people, and 96 people were killed (Hoscilo et al., 2015).

A better understanding of how more extreme weather impacts above-ground net primary production (ANPP) is needed to anticipate impacts on livelihoods better. Previous studies that sought to increase that understanding have been predominantly carried out in the United States. For semi-arid grassland sites, rain-shelter experiments show that fewer but larger rain events resulted in higher ANPP as compared to plots that receive the same rainfall more frequently. The soil moisture showed that heavy rains caused overall higher soil water content because more water infiltrated into the ground (Heisler-White et al., 2008). Fay et al. (2008) also used the rain-shelter experiment to examine how the variation in the interval between rainfall events, the quantity of total rainfall and individual event size affected soil water content, leaf photosynthesis, soil respiration and ANPP. The result shows significant differences in ANPP and soil respiration differ in the interval between rainfall events and rainfall total quantity which sharing the same individual event size. This study suggests that the ecosystem response to extreme rainfall patterns is likely depend on the specific ways that these three elements are combined during each season. Even if the impact of more extreme rainfall

varies between different ecosystems, but understanding these impacts is important for predicting how more extreme rainfall will change the ecosystem.

Research in other parts of the globe has shown that more extreme patterns of rainfall can cause both increases and decreases in vegetation productivity. Based on a review of existing literature, Zeppel et al. (2014) found that redistribution of rainfall might occur across and within seasons which may lead to soil water content that affect plants. This study combined manipulative and observational studies to focus on manipulative experiments and modeling response of plants to the altered precipitation seasonality and extreme distribution of precipitation. They examined impacts of precipitation redistributed on plants processes which included leaf water potential, stomatal conductance, soil fluxes and ANPP. Also, they assessed the response of plants to changes in seasonality precipitation. The results showed that extreme precipitation to ANPP led to increases in water-limited sites and increased soil water content. Also, extreme precipitation at mesic sites caused a decrease in ANPP and soil water content. They also found that seasonal changes in precipitation are frequently causing water stress, decrease biomass and changes in phenology though the impacts are depending on changes in precipitation per season and per location.

Apart from field experiments, also satellite data have been used to investigate the impacts of extreme precipitation patterns on ANPP. Zhang et al. (2013) used satellite measurements of greenness and long-term rain gauge data from the 11 United State Department of Agriculture (USDA) experimental stations across United States. An assessment was done to study the impacts that occur on vegetation productivity which is caused by interannual variability of precipitation by using a seasonal integral of a remotely sensed vegetation index as a proxy for ANPP. More extreme seasonal distribution of precipitation resulted in ANPP increases in xeric grassland sites, but in ANPP decreases in mesic grasslands.

While research in other parts of the globe have shown that more patterns of rainfall can cause both increases and decreases in vegetation productivity, for East Africa; such studies are lacking. Nonetheless, given expected increases in extreme rainfall events and increases in dry-spells here and the strong dependence of livelihoods on vegetation productivity, it is important to understand how such changes may impact vegetation productivity.

1.2. Research objectives

The main objective is to evaluate if within-season rainfall distribution, as captured by extreme precipitation indices, can improve the prediction of seasonal vegetation productivity as compared to total seasonal rainfall.

Specific objectives

➢ To extract multi-year indicators of seasonal above-ground net primary productivity (ANPP) and total seasonal rainfall using season definitions derived from NDVI and station-rainfall time series.
➢ To evaluate to what extent total seasonal rainfall can explain the interannual variability of the ANPP proxy.
➢ To extract time series of extreme seasonal indices from daily rainfall station data and assess if and to what extent these can explain rain use efficiency (ANPP divided by seasonal rainfall)

2.   STUDY AREA AND DATA

2.1.   Study area and rainfall data

The seasonality in Kenya is characterized by bimodal and unimodal rainfall regimes (Herrmann & Mohr, 2011). A large part of the country experiences two rainfall seasons known as long rains (March to June) and short rains (October to December). Some other parts of the country such as central highlands have a more unimodal rainfall regime (Owiti, 2012) with a single rainfall season per year.

The topography of the study area (Figure 1a) defines the country as follows; the central region is higher and crossed with the Great Rift Valley while on Eastern region the topography rises gradually from a narrow coastal plain in series of plateaus. The study area contains several land use and land cover categories as shown in (Figure 1b). In Kenya most part of the country such as Northern and Northern Easter areas are covered with grassland with shrubs and trees while on Western part cropland is dominant. The economic activities practices for the rural livelihood in Kenya is livestock keeping including camels, goats, sheep and cattle (Vrieling et al., 2014). In the wetter areas of the country crop cultivation is increasing and played the role of economic change strategy (Rufino et al., 2013).

The study area was defined based on the availability of multi-year data from rainfall stations in Kenya. Data were searched for rainfall stations within Kenya which have a multi-year availability of daily rainfall data. The daily rainfall series analysed were compiled from Joint Research Centre (JRC) of European Commission (Alterra et al., 2013), Kenya Meteorological Department (KMD), ACRE Africa, International Livestock Research Institute (ILRI) and Centre for Training and Integrated Research in Arid and Semi-Arid Lands Development the dataset is available through free download from CETRAD website (http://wlrc-ken.org/). Figure 1c shows the geographical locations of the retained stations together with their sources.

Criteria used to select rainfall stations were 1) the availability of daily rainfall data for at least 10 years or more with less than 5% of the daily observations lacking, 2) a relatively homogeneous natural land cover (e.g. savannah, forest) in the vicinity of the station. If more than 5% of the observations for a given season, the particular year was excluded from analysis. The stations with less than ten years of data meeting the threshold were discarded. Based on the criteria, a total of 299 long rains and 294 short rains seasons of daily precipitation from 22 stations were used for further analysis (Table 1).

Based on these daily rainfall data from 2001-2016, the study area was classified into three climatic zones based on the average annual rainfall of these rainfall stations. Stations having average annual rainfall between 150-550 mm were classified as arid, 550-900mm, semi-arid and 950-1400mm semi-humid (Dr.Kirubi & Dr.Kahuthia-Gathu, 2012) Table 1.

Table 1. Characteristics of the rainfall stations used in the study area with their sources and availability of data

| Station name | Coordinates | | Available data range | Source | Total number of seasons 2001-2016 | | Average annual rainfall (mm) | Climate |
	Latitude	Longitude			LR	SR		
Kapiti Farm	-1.634003	37.147621	2001-2016	ILRI	16	16	513	Arid
Elgon Downs Farm	1.06275	34.85658			16	13	1,162	Semi-humid
Homabay Water Supply	-0.52472	34.45662			10	11	825	Semi-arid
Kalalu LRP	0.08134	37.16475			15	16	699	Semi-arid
Muriranjas Vocational	-0.74498	36.97361	2001-2016	Acre Africa	10	11	1072	Semi-humid
Tenri Koatec	-0.47247	37.55396			12	11	971	Semi-humid
Timau Marania	0.08781	37.45881			16	16	1,052	Semi-humid
Archers Post	0.63707	37.66758			16	16	359	Arid
Kalalu (NRM)	0.08134	37.16475	2001-2016		15	16	771	Semi-arid
Munyaka (NRM)	-0.18355	37.05923		CETRAD	13	16	658	Semi-arid
Naro Moru Met STN	-0.1706	37.21392			16	16	1505	Semi-humid
Nakuru	-0.27	36.07			14	13	944	Semi-humid
Lamu	-2.27	40.9			11	11	588	Semi-arid
Voi	-3.4	38.57			14	13	479	Arid
Mombasa	-4.03	39.62		KMD and JRC	14	14	862	Semi-arid
Lodwar	3.1167	35.64			14	13	227	Arid
Marsabit	2.32	37.98			13	11	533	Arid
Wajir	1.75	40.07	2001-2015		14	13	321	Arid
Narok	-1.13	35.83			13	11	582	Semi-arid
Mandera	3.95	41.87			11	11	192	Arid
Garissa	-0.48	39.63			12	13	258	Arid
JKIA	-1.32	36.82			14	13	645	Semi-arid
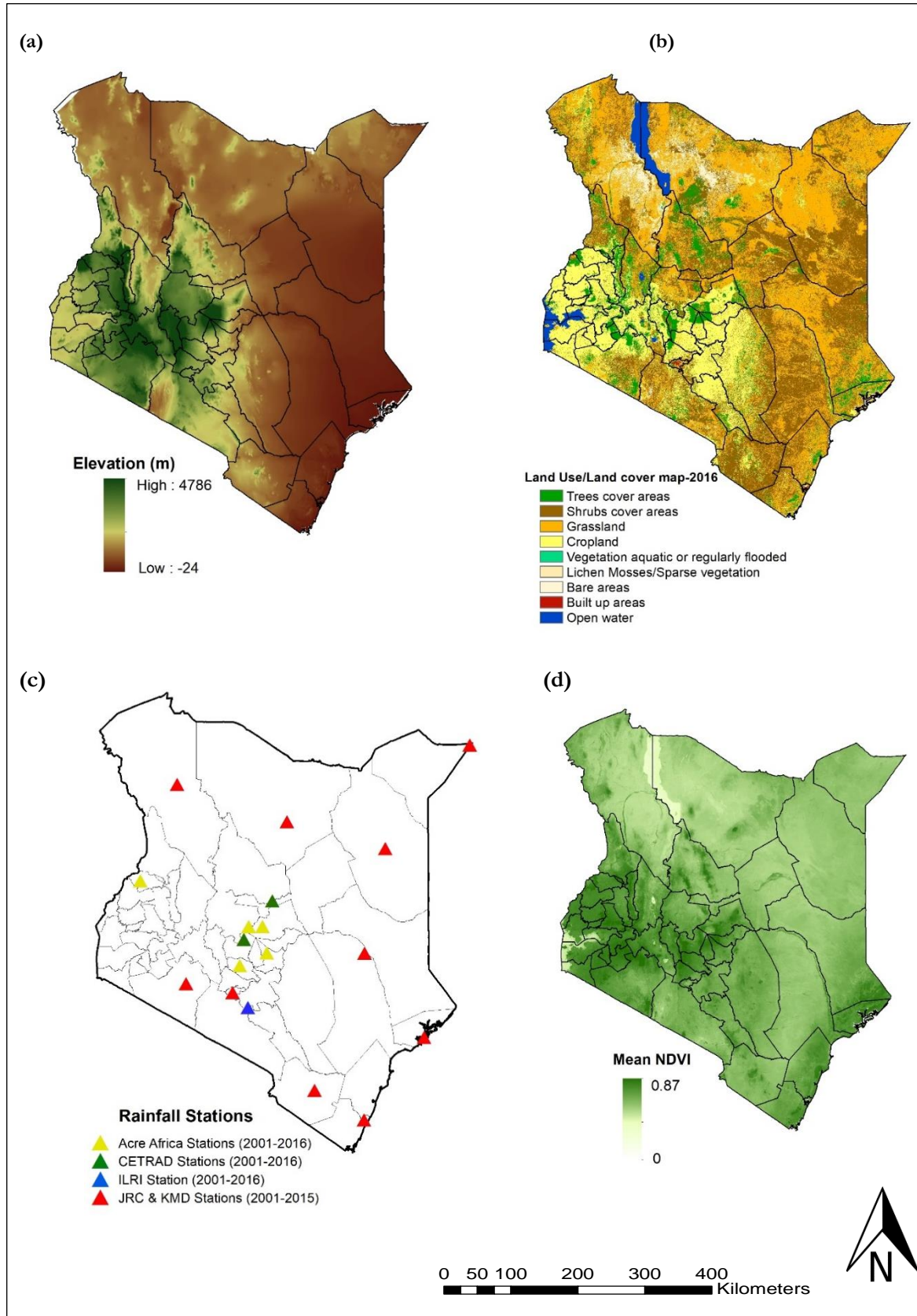
Figure 1. Maps of the study area (Kenya) showing; (a) Elevation (source: https://earthexplorer.usgs.gov/) (b) Land use/land cover for the year 2016 (source: http://2016africalandcover20m.esrin.esa.int/) (c) The distribution of stations with daily time series selected in this study and the corresponding source for each station; and (d) The mean NDVI (2001-2016) from 10-day eMODIS composites Remote sensing data

2.1.1. NDVI Time series

To estimate the interannual variability in ANPP, in this study time series of NDVI from the Enhanced Moderate Resolution Imaging Spectroradiometer (eMODIS) version 5 product was used. This product is made by the United States Geological Survey (USGS); based on MODIS data acquired by the Terra satellite. Although version 6 of eMODIS based on the Aqua satellite is also available, was observed with noise problem in those data and consequently, it was decided to use version 5. The eMODIS product consists of 10-day (dekad) maximum value NDVI composites at 250m resolution (Jenkerson et al., 2008). Temporal smoothing is applied to minimize atmospheric effects that degrade the NDVI signal. This is achieved with the Swets algorithm which applies a weighted least-squares regression to a moving temporal window for each pixel time series assigning largest weights to local peaks in the NDVI profile (Swets at al., 1999). The smoothed eMODIS product is available and can be freely downloaded from the year 2001 onwards. For the East Africa window, a set of images from the year 2001 to 2016 was downloaded and used in this study.

2.1.2. Ancillary data

Google Earth imagery was used for selecting homogeneous areas with similar characteristics and stable natural vegetation using visual interpretation.

2.2. Software

The following software was used:

- ArcGIS version 10.5 was used for interact and create maps, i.e. analyse geographical data, view and editing.
- Microsoft Excel – Calculating and analysing large time series, statistical analysis and plots
- IDL – Extracting and calculating extreme rainfall indices

3.   METHODS

3.1.   Extracting seasonal ANPP and rainfall

3.1.1.   Defining rainfall seasonality regimes

This study examines rainfall and vegetation productivity within a season. This requires a definition of the season, i.e. when does it start and when does it end. This seasonality is not the same throughout the study area, because in some regions rains may start or end earlier than in other parts. Moreover, for a single location these definitions can be different for NDVI and rainfall; vegetation usually greens-up after the rains have raised soil moisture content, and also remains green after the last rains of the season have taken place.

Before defining the start and end of the season of rainfall, a preliminary analysis was performed to evaluate for each station if the average rainfall distribution within the year shows a clear seasonal pattern. This was done by calculating the seasonality index (SI) as follows (Walsh & Lawler, 1981):

$$SI = \frac{1}{R} \sum_{n=1}^{n=12} \left| X_n - \frac{R}{12} \right| \tag{1}$$

where X_n is the monthly average rainfall for each month n and R stands for average annual rainfall. The index has a minimum value of 0 if all the months have an equal amount of rainfall, and a maximum value of 1.83 if all the rainfall occurs in a single month. The 0.60 value has been set as the threshold between clear and limited seasonality. The SI was calculated for the multi-year average (2001-2016) for each station time series and classified according to Table 2.

Table 2. Seasonality index classes

SI class limits	Rainfall regime
<0.60	Precipitation spread throughout the year
0.60 – 0.80	Seasonal
>0.80	Markedly seasonal with a long dry season

3.1.2.   Seasonal temporal integration periods for ANPP

Different approaches exist to perform phenological analysis from NDVI time series (de Beurs & Henebry, 2010) which allows obtaining a spatial-temporal representation of vegetation seasonality. This study used the outcome of an approach that was first published by Meroni et al. (2014) and is well capable of dealing with the bimodal seasonality that is common to East Africa. The phenological analysis was applied using the NDVI time series from the eMODIS data to estimate the start-of-season (SOS) and end-of-season (EOS) and as such to identify the key period when biomass develops.

First, the NDVI time series was only evaluated if at least 60% of the 10-day composites had valid NDVI values for land and if the dynamic range (defined as the difference between the 95th and 5th percentile of the full-time series value) was greater or equal than 0.10 NDVI units. If the pixel did not meet this condition, it was masked out. Then the Lomb normalized periodogram (algorithm used for detecting and characterizing periodic components in unevenly sampled time series (Lomb, 1976; Scargle, 1982; VanderPlas, 2017) was applied to evaluate per-pixel if the overall behavior is bimodal or unimodal. Using a 'median year' and the estimated uni- or bi-modality, breakpoints between seasons were set at the NDVI minima. A parametric

double hyperbolic tangent model was then fitted to the data of each season and pixel. The SOS was estimated for each season per year as the moment when the fitted NDVI model exceeded 20% of the local growing amplitude (i.e. between minimum NDVI before green-up and maximum NDVI of that season), and EOS as the moment when it falls below 80% of the decay amplitude (i.e. between maximum NDVI of the season and the following minimum NDVI after decay). Finally, the multi-annual average and standard deviation of SOS and EOS were calculated per pixel (Vrieling et al., 2016).

Subsequently, to account for the interannual variability in SOS and EOS, half a standard deviation was subtracted from the per-pixel SOS estimates, and half a standard deviation was added to the EOS estimate. The resulting dates were translated into a number from 1 to 36, reflecting the 10-day period (dekad) that the obtained SOS and EOS dates represent, i.e. 1 being 1-10 January (Vrieling et al., 2016). These NDVI derived SOS and EOS dekads are referred to here as SOS_N and EOS_N.

To obtain a proxy measure of ANPP, per season and year, the dekad NDVI values were accumulated between the site-specific SOS_N and EOS_N dates. The step can be expressed as:

$$CumNDVI_s = \sum_{t=SOS_N}^{t=EOS_N} NDVI_t \qquad (2)$$

where $CumNDVI_s$ is the cumulative NDVI value for each season per pixel, **s** represents a long rain or short rain season in a specific year, and $NDVI_t$ is the pixel value of one dekad (**t**) within that season (as defined by SOS_N and EOS_N). The cumNDVI, values were then used as a proxy for the above-net primary productivity (ANPP). Figure 2 shows a temporal graph of Archers Post pixel as an example of cumulative NDVI between SOS and EOS for long and short rains.
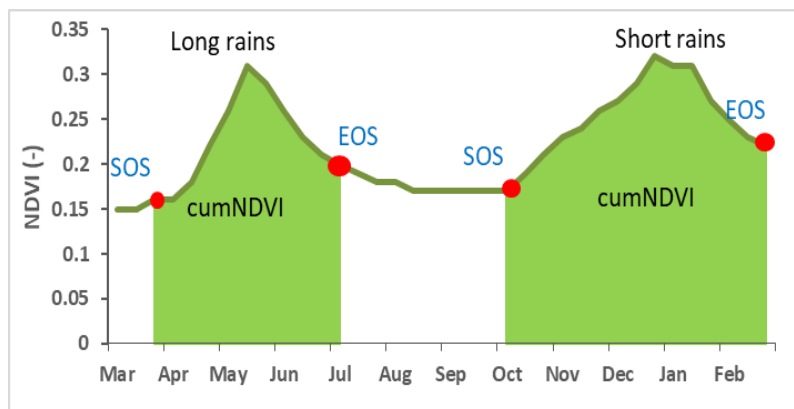
Figure 2. Temporal graph of Archers Post showing the start of the season (SOS) and end of the season (EOS) derived separately for the long rains and short rains. The cumNDVI is the cumulative value of NDVI between SOS and EOS is the green area under the curve. The red dots correspond to the start and end dates for long and short rains season

3.1.3. Seasonal temporal integration periods for rainfall

In this study, the approach to extract the start and end of the rainfall season is based on Liebmann et al. (2012) who adapted the approach originally published by Liebmann & Marengo (2001). Dunning et al. (2016) applied the same approach to assess precipitation seasonality across the African continent. The Liebmann's rule defines the SOS as the moment when daily precipitation consistently exceeds its local annual daily average and ends when daily precipitation drops below that value. In this study, the rule was applied to the precipitation climatology of the study area using daily data (2001-2016) per each station.

First, the long-term daily average (e.g. the average of all 1 January observations) for each day of the year and the long-term annual mean daily average (i.e. the average of all observations in the 2001-2016 window) are calculated. From 1 January the long-term daily average minus the long-term annual mean average is summed: this process is called anomalous accumulation. This can be expressed as:

$$A(d) = \sum_{i=1Jan}^{d} R_i - R$$

(3)

where $A(d)$ is anomalous accumulation, R_i is the long-term daily average while R is the long-term annual mean daily average and i ranges from 1 January to the day (d) for which the calculation applies.

The first day past the minimum value of anomalous accumulation marks the SOS, while the EOS is defined as the day when the anomalous accumulation reaches its maximum value as shown in Figure 3a. The same rule was applied to individual years to retrieve the annual SOS and EOS dates. Accounting for the interannual variability while reducing the chance of overlap between seasons, half of the standard deviation was subtracted from the average SOS dates and added to the EOS dates Figure 3b. This is the same as done for NDVI-based on SOS and EOS (Section 3.1.2).

For each station data, the total seasonal precipitation was then calculated per season using the SOS and EOS dates. The step can be expressed as:

$$CumP = \sum_{t=SOS_R}^{t=EOS_R} P_t$$

(4)

where $CumP$ is the cumulative precipitation for each season, the SOS_R and EOS_R are the start and end of season dates as derived from the station rainfall data (R for rainfall), and P_t is the rainfall during one day (t) belonging to the season.
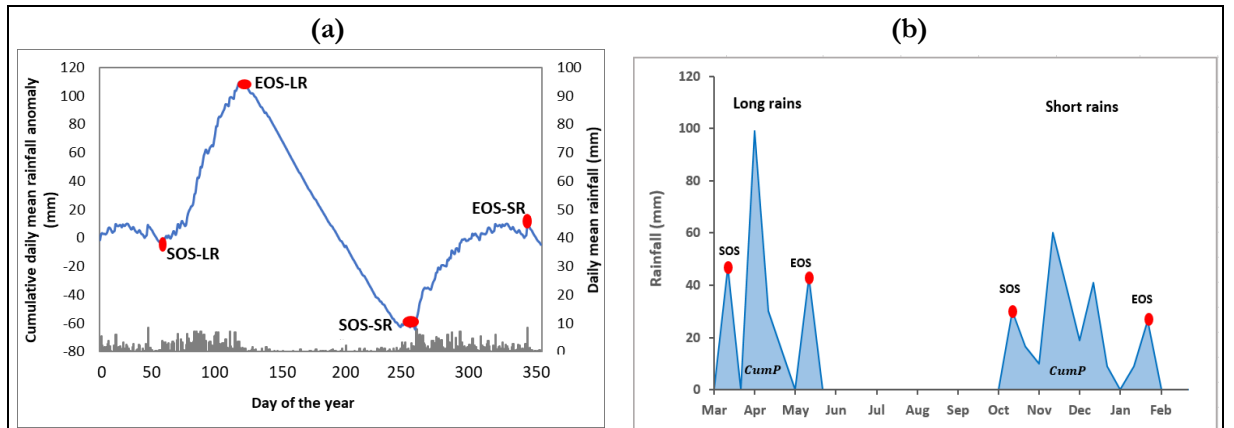
Figure 3. Kapiti Farm station: a) Climatological cumulative daily mean rainfall anomaly (blue line) and daily mean rainfall (grey bars) for each day of the year averaged over 2001 – 2016. The descending lines between the seasons are the dry periods. b) $CumP$ is the cumulative value of rainfall between SOS and EOS under the blue curve. The red dots correspond to the start and end dates for long and short rains season.

3.2. Evaluation of interannual variability of ANPP and total seasonal rainfall

To assess to what extent the interannual variability in total seasonal rainfall can explain ANPP variability a linear regression model was used separately for long and short rains for all selected rainfall stations and corresponding pixels. Each station combination was analyzed separately by examining their 10-16 year variability in rainfall and ANPP.

In addition, to evaluate the response of ANPP to total seasonal rainfall between stations, the stations were split into three groups with the similar climatic condition and labeled as arid areas, semi-arid areas and semi-humid areas into a regression analysis for both the long and short rains. All stations were combined in one analysis to determine how much of interannual variability is explained in long and short rains.

Further analysis was done using a one-way ANOVA to test whether there was a significant difference between both the long and short rains seasons for the three climatic groups, i.e. arid, semi-arid and semi-humid areas. Among the groups, the mean values of each group were compared per season using a Games-Howel post hoc test.

3.3. Extreme indices

An extreme index provides information about the within-season distribution of weather variables such as precipitation (IPCC, 2012). A core set of 27 descriptive extreme indices has been defined by the Expert Team on Climate Change Detection and Indices (ETCCDI), in order to uniformly monitor changes in extreme climate and weather (WMO, 2009).

While usually extreme indices are calculated in relation to a 30-year reference to climatological period, in this study, the long-term rainfall data from the stations have been used as the statistical basis to assess extreme indices. This study used the extreme indices as proposed by Zhang et al. (2013), who used similar indices and found them have explanatory power for ANPP variability. The set of extreme precipitation indices considered for this study include R95p%, R95pTOT, CDD and SDII as defined in Table 3. CDD is an indicator of the length of a dry spell, SDII express the intensity of extreme precipitation, R95pTOT shows seasonal precipitation due to wet days (daily rainfall exceeding the 95th percentile) and R95% represents the fraction of total precipitation due to days with rainfall amount above >95th within a season.

Table 3. The extreme indices definitions

Index	Abbreviation	Definition	Units
1.	R95pTOT	Precipitation due to wet days (daily rainfall >95th percentile)	mm
2.	R95p%	Precipitation fraction of total precipitation due days with rainfall amount >95th percentile	%
3.	SDII	Simple daily intensity index:	mm/d
4.	CDD	Maximum number of consecutive dry days (<1 mm)	days

Source: ECA&D (2017), full definition and other precipitation indices are available from
http://eca.knmi.nl/indicesextremes/indicesdictionary.php

The extreme indices were calculated per season using daily precipitation observations from each station. An extreme index was only calculated for a season if no more than 5% of the rainfall data for a specific season within the period SOS_R and EOS_R was missing. Any missing observations were simply discarded, i.e. they were not counted as a dry or wet day, nor incorporated in the calculation of the 95th percentile. For the

dataset with more daily precipitation observations were missing for a specific season, the extreme index was set to a missing value for that season for that year.

3.3.1. Response of rain use efficiency to extreme indices

To account for the seasonal rainfall amount on ANPP, the ANPP was normalized by dividing it by total seasonal rainfall. This normalized ANPP can be defined as the rain use efficiency (RUE).

This study used simple linear regression and a Pearson correlation coefficient analysis to assess the relationship between RUE and the extreme indices. The analysis was done separately for each station with each one of the extreme indexes; R95p%, R95pTOT, CDD and SDII to assess to what extent each of these indices individually can explain the variability in RUE. The analysis was further done by combining stations with same climatic characteristics into three groups arid, semi-arid and semi-humid areas and for each group, one regression analysis was attempted to assess if a grouping of similar locations can improve the explanatory power of these extreme indices on RUE.

Further analysis was done using a natural logarithm transformation regression model on stations grouped as a climatic zone (i.e. arid, semi-arid and semi-humid areas) to improve the non-linear relationship result observed from simple linear regression. This method of natural logs transformation was first done by adding a constant value of 1 to each value of a variable to reduce an error caused by observations with zero values. Therefore, transformation was done as;

LN(1+x)   5

where **LN** returns the natural logarithm of a number **x** which both RUE and extreme index and **1** is the constant value.

4.   RESULTS

4.1.   Temporal integration of seasonal ANPP and rainfall

4.1.1.   Spatial variability of rainfall seasonality regimes

The seasonality index (SI) was classified into three classes. For the 22 retrieved stations (Table 1), three stations with SI below 0.60 were discarded because their more uniform rainfall distribution does not allow to clearly separate wet and dry seasons. Table 4 shows the SI of each retained station.

Figure 4 shows the temporal graphs for two stations that represent a different precipitation distribution regime (SI). The temporal behavior of NDVI and rainfall clearly indicate a bimodal seasonal cycle. Figure 4 shows the correspondence between rainfall and NDVI, where NDVI mostly reach a maximum after the peak of the rainy season. Figure 4a Kapiti Farm station is consistently very dry throughout the dry months and has short rainfall seasons while Figure 4b Munyaka (NRM) station has longer rainy seasons with a shorter dry period.
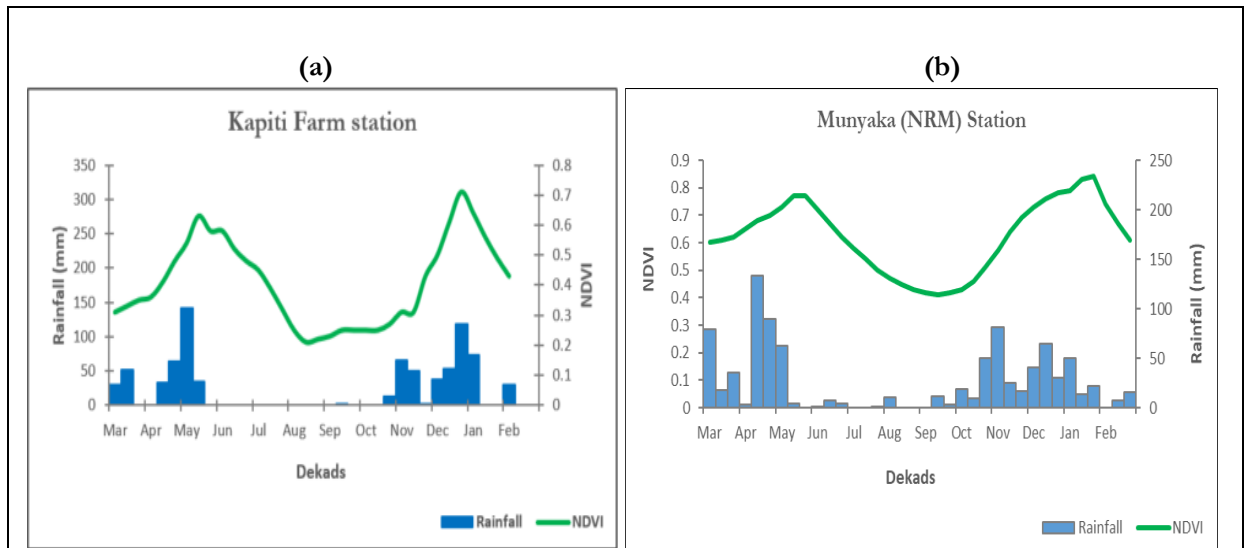
Figure 4. Temporal graphs representing a year average of the two precipitation regimes in the study area (a)Kapiti Farm station with SI 1.00, (>0.80) markedly seasonal with the long dry season (b) Munyaka (NRM) station with SI 0.68, (0.60-0.80) Clear seasonality

4.1.2.   Derived start and end of season dates for ANPP and rainfall

For the analysed stations the SOS_R dates for the long rains are from early March to late May for most stations except for Narok which start early February. Few stations the EOS_R dates are observed early June except for Lamu which is mid-July. The SOS_R dates for the short rains are from early mid-August to early September for other stations and EOS_R dates are late December for most stations except for few which ends late November and January (Table 4). For some stations, a correspondence between SOS_R/EOS_R and SOS_N/EOS_N dates were observed for the long rains. In short rains, some stations have been observed with the large gap between SOS_R/EOS_R and SOS_N/EOS_N dates.

Table 4. The table indicates the start and end dates for the long and short rains season of precipitation and cumulative NDVI, classification of the seasonality index (SI) as assessed at each rainfall station

Station name	SI	P_{LR}		P_{SR}		cumNDVI$_{LR}$		cumNDVI$_{SR}$	
		SOS$_R$	EOS$_R$	SOS$_R$	EOS$_R$	SOS$_N$	EOS$_N$	SOS$_N$	EOS$_N$
Kapiti Farm	1.00	01 MAR	31 MAY	01 OCT	31 JAN	21 MAR	10 AUG	21 OCT	20 FEB
Elgon Downs Farm	0.61	21 MAR	30 JUN	21 AUG	30 NOV	11 APR	10 OCT	21 OCT	20 FEB
Kalalu LRP	0.75	21 MAR	20 JUN	21 AUG	10 DEC	11 APR	30 SEP	01 NOV	28 FEB
Muriranjas Vocational	0.67	21 MAR	10 JUN	11 OCT	31 DEC	10 APR	31 AUG	21 OCT	28 FEB
Tenri Koatec	0.81	11 MAR	10 JUN	01 OCT	20 DEC	01 APR	10 AUG	31 OCT	28 FEB
Timau Marania	0.81	11 MAR	20 MAY	11 OCT	31 DEC	01 APR	31 JUL	31 OCT	28 FEB
Archers Post	1.04	11 MAR	31 MAY	01 OCT	31 DEC	21 MAR	10 JUL	31 OCT	20 FEB
Kalalu (NRM)	0.74	20 MAR	30 JUN	21 AUG	10 DEC	11 APR	30 SEP	01 NOV	28 FEB
Munyaka (NRM)	0.68	01 MAR	31 MAY	21 SEP	31 DEC	21 MAR	20 AUG	11 OCT	28 FEB
Lamu	0.60	01 MAR	20 JUL	11 AUG	30 NOV	21 MAR	10 AUG	01 NOV	20 FEB
Voi	0.85	21 MAR	20 MAY	21 OCT	31 DEC	01 APR	10 AUG	21 OCT	28 FEB
Mombasa	0.63	01 MAR	20 JUN	11 AUG	10 DEC	21 MAR	30 SEP	21 OCT	10 FEB
Lodwar	0.97	21 MAR	31 MAY	21 AUG	20 DEC	01 APR	31 JUL	11 OCT	31 JAN
Marsabit	0.90	01 MAR	20 MAY	01 SEP	10 DEC	01 APR	10 AUG	21 OCT	20 FEB
Wajir	1.03	11 MAR	10 MAY	21 SEP	30 NOV	01 APR	10 AUG	21 OCT	28 FEB
Narok	0.67	11 FEB	20 MAY	01 AUG	20 DEC	01 APR	10 SEP	01 NOV	28 FEB
Mandera	1.05	01 MAR	10 JUN	11 OCT	20 DEC	21 MAR	20 JUN	31 OCT	10 JAN
Garissa	1.01	21 MAR	20 MAY	11 OCT	31 DEC	01 APR	10 AUG	21 OCT	28 FEB
JKIA	0.73	01 MAR	20 JUN	21 AUG	31 DEC	01 APR	10 AUG	11 OCT	28 FEB

Vegetation green-up generally responds after the first rains have raised the soil moisture availability and are consequently later than the first rainfall. Also, vegetation remains green for some time after the last rains of the season have taken place. In Figure 5a the Timau Marania station temporal graph has been used as an example to show the results of how NDVI showed a close correspondence to rainfall fluctuations in both seasons while Figure 5b Kalalu NRM station shows the large deviation between rainfall and NDVI.
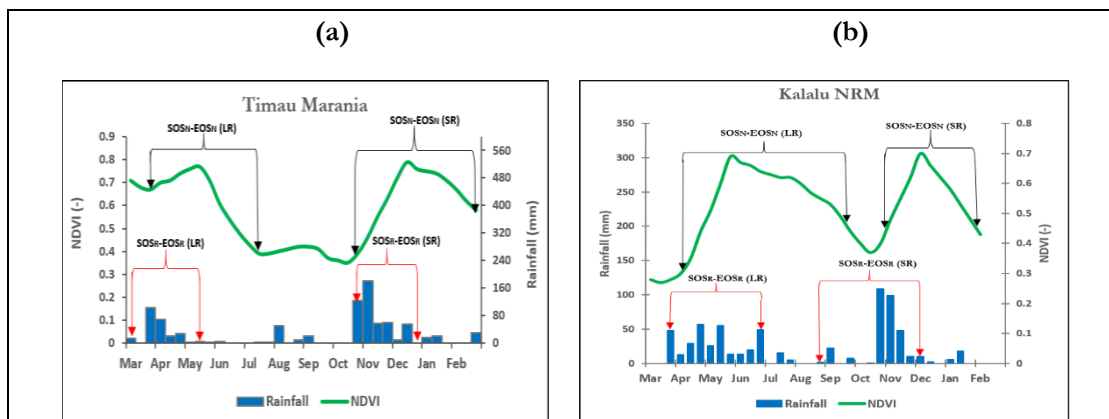
Figure 5. Temporal graphs showing average rainfall and NDVI for (a) Timau Marani and (b) Kalalu NRM the black arrows indicating the results of phenological analysis of NDVI for SOS$_N$ and EOS$_N$ dates and red arrows for rainfall SOS$_R$ and EOS$_R$ dates for the long rains and short rains

4.2. Relationship between ANPP and seasonal rainfall

4.2.1. Response of ANPP to seasonal rainfall per station

Seasonal rainfall can explain part of the ANPP variability, but the extent to which this is feasible differs greatly between stations. For most stations, less than 50% of the variability is explained (Table 5). This means that other factors (e.g. the rainfall distribution within the season) could be important determinants of the ANPP variability.

Table 5 shows how much of interannual variability in cumNDVI can be explained by total seasonal rainfall for each station and for both the long and the short rains. As for Figure 6, important differences can be observed between stations and between seasons (scatterplots for other stations are presented in Appendix I). Out of all 38 station-season combinations, only for 10 cases more than 50% of the cumNDVI variability could be explained by rainfall. Only for two stations (Archers Post and Lamu, Table 5 and Figure 6ab), this was the case for both long and short rains. The highest R^2 (0.82) was observed for Voi (Figure 6c) during the short rains, while Lodwar had the lowest R^2 (0.06), both for long and short rains (Figure 6d). When combining both seasons in a single analysis for each station, Lamu shows the highest R2 (0.75) among all stations (Figure 6b, Table 5)

Across all 19 stations, for both the long and the short rains, total seasonal rainfall explains on average less than 50% of the cumNDVI variability (Table 5, Appendix I). While for some stations and seasons a total seasonal rainfall is a good predictor for cumNDVI, much of the cumNDVI variability is not explained by seasonally cumulated rainfall alone.

Table 5. R^2 between cumNDVI and seasonal rainfall for individual station for long and short rains

Station name	Long rains	Short rains	LR&SR
Kapiti Farm	0.27	0.73	0.38
Elgon Downs Farm	0.13	0.28	0.02
Kalalu LRP	0.50	0.38	0.43
Muriranja Vocational	0.33	0.24	0.02
Tenri Koatec	0.19	0.17	0.18
Timau Marania	0.34	0.10	0.31
Archers Post	0.51	0.65	0.59
Kalalu (NRM)	0.44	0.61	0.48
Munyaka (NRM)	0.55	0.20	0.41
Lamu	0.77	0.61	0.75
Voi	0.33	0.82	0.61
Mombasa	0.36	0.39	0.32
Lodwar	0.06	0.06	0.10
Marsabit	0.62	0.44	0.50
Wajir	0.41	0.51	0.44
Narok	0.08	0.31	0.32
Mandera	0.13	0.49	0.56
Garissa	0.19	0.14	0.18
JKIA	0.13	0.46	0.24
Average	0.37	0.40	0.36

Legend:

▮	Maximum 0.90
▯	Minimum 0
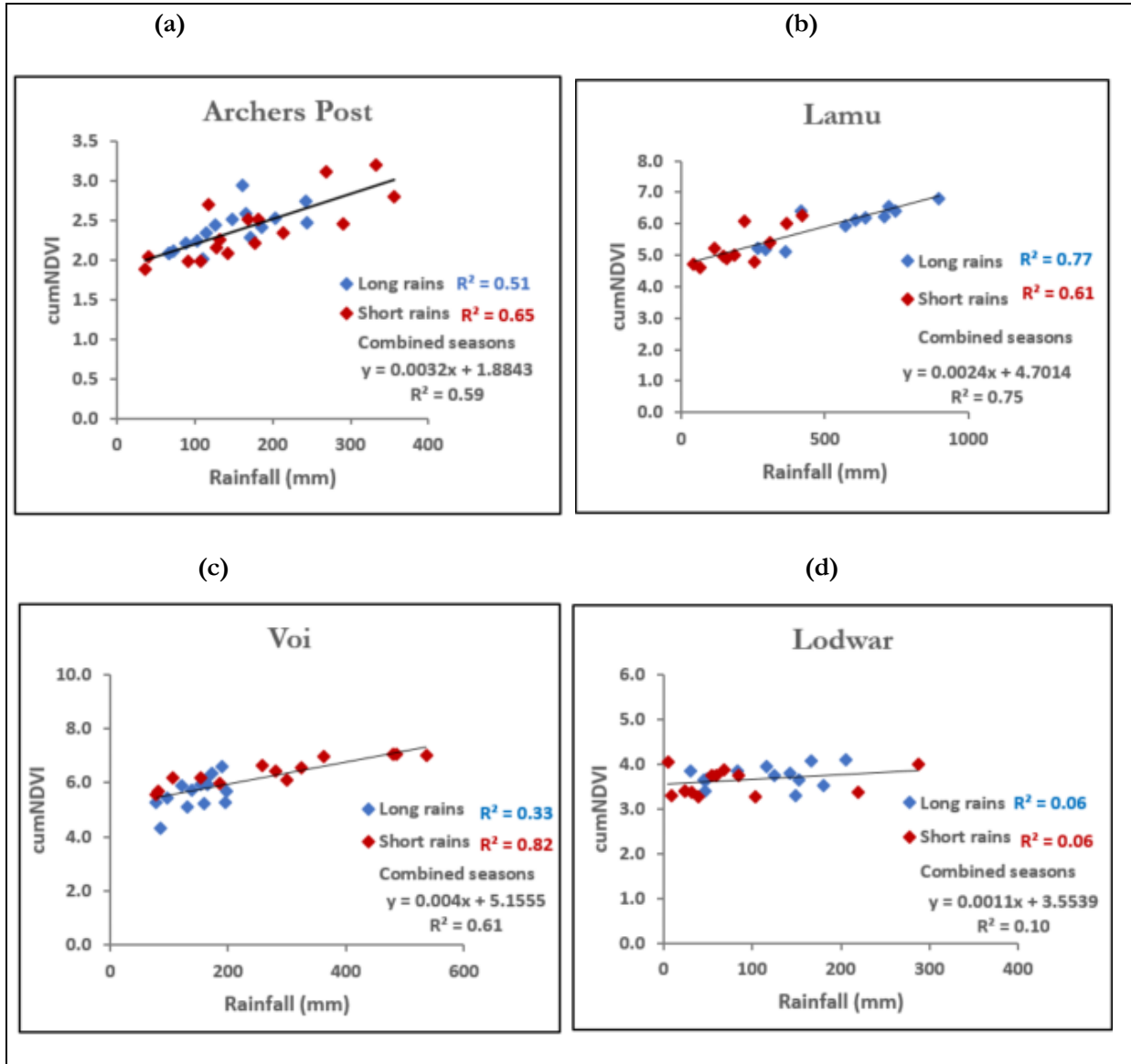
Figure 6. Scatterplots representing the stations with the highest correlation between the cumNDVI and total seasonal rainfall and to show the spread in correlation from low to high correlation for; (a) Archers Post, (b) Lamu, (c) Voi and (d) Lodwar

4.2.2. Response of ANPP to seasonal rainfall per grouped stations

The amount of explained variability did not increase when grouping observations according to climatic zones. Table 6 shows how much of interannual variability in cumNDVI can be explained by total seasonal rainfall for a grouped location for both the long and the short rains. For the three groups (arid, semi-arid, and semi-humid), the variability of R^2 0.31 was explained in arid areas during the short rains season (Figure 7a). For the other groups, the amount of variability explained is even less (Figure 7, Table 6). A combined of all stations and seasons in a single analysis resulted in an overall R^2 of 0.37 (Figure 7d)

Table 6. R² between cumNDVI and seasonal rainfall combined in three groups per location for long and short rains

Location	Long rains	Short rains	LR&SR
Arid	0.31	0.28	0.28
Semi-arid	0.09	0.12	0.12
Semi-humid	0.06	0.04	0.04
All stations	0.37	0.37	0.37

Legend:

Maximum 0.90
Minimum 0

Figure 7. Scatterplots showing the relationship between cumNDVI and total seasonal rainfall for stations grouped; (a) arid areas, (b) semi-arid areas (c) semi-humid areas and (d) all stations

Figure 8 representing the climatic zone groups per seasons showing that there was a statistical difference between the groups. A Post-hoc comparison using the Games-Howell test shows there is evidence that at least one group is significantly mean different from the rest during the short rains. Between the mean arid and semi-humid areas was significant (P=0.197). Also, between the mean semi-arid and semi-humid areas was significant (P=0.085). However, the mean between arid and semi-arid areas was no significant difference (P=0.722) as presented by box plots and whisker (Figure 8, Appendix II)
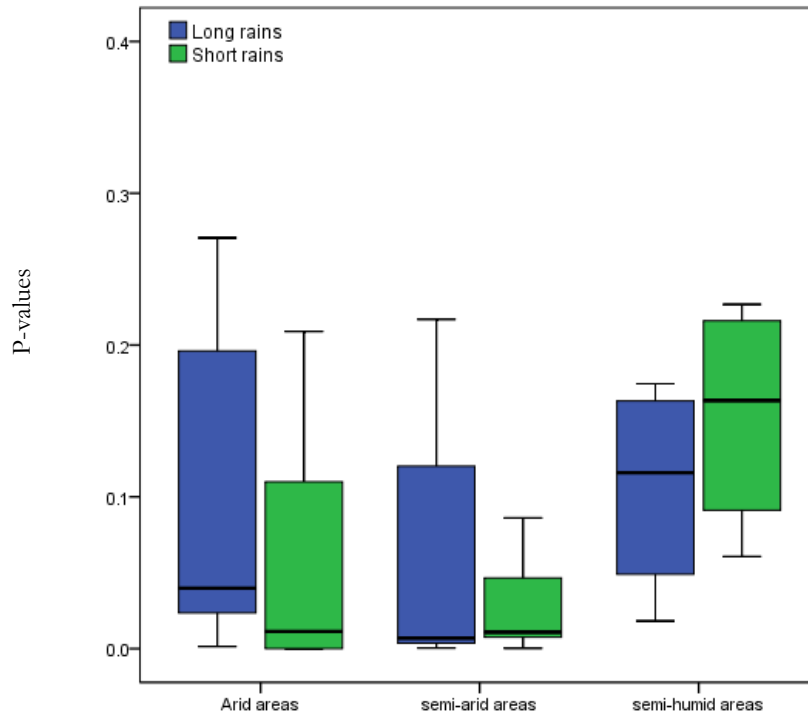
Figure 8. A box plot and whisker of a grouped climatic zone stations at significance difference P < 0.05

4.3. Response of RUE to extreme precipitation indices

Table 7 shows how much of RUE variability is explained by extreme indices for each station for both long and short rains. For all extreme indices, R95pTOT is explaining over 60% of the RUE variability for 15 out of 19 stations in long rains and 11 for short rains. This index explains more of the ANPP variability as compared to total seasonal rainfall. For all the stations the Pearson correlation coefficients between R95pTOT and RUE were negative for both seasons (Appendix III). Only six stations (Kapiti Farm, Kalalu NRM, Munyaka NRM, Lamu, Voi and JKIA) more than 60% of the RUE variability could be explained by R95pTOT for both the long and short rains. The highest R^2 (0.89) was observed for Voi during the long rains, while lowest R^2 was observed in Narok (0.07) the long rains and in Wajir (0.05) for the short rains.

The Pearson correlation coefficient between the CDD and RUE was positive for all stations (Table 7). For Narok, no correlation ($R^2=0.00$) was observed between CDD and RUE for either season. Only three stations explain above 60% of RUE variability in one of the seasons (Muriranja Vocational and Mombasa) and four stations explain 50% RUE variability Kapiti Farm, Lamu, Lodwar and Wajir which is for both seasons long and short.

Table 7. R² for each station representing the relationship between RUE to extreme indices per both seasons long and short rains in the study area

Station name	CDD		SDII		R95%		R95pTOT	
	LR	SR	LR	SR	LR	SR	LR	SR
Kapiti Farm	0.12	0.54	0.11	0.43	0.16	0.55	0.72	0.71
Elgon Downs Farm	0.00	0.21	0.33	0.62	0.52	0.61	0.80	0.54
Kalalu LRP	0.01	0.26	0.38	0.63	0.42	0.54	0.62	0.69
Muriranja Vocational	0.01	0.60	0.06	0.13	0.03	0.24	0.19	0.67
Tenri Koatec	0.26	0.08	0.41	0.62	0.29	0.34	0.24	0.74
Timau Marania	0.05	0.24	0.54	0.77	0.33	0.61	0.69	0.85
Archers Post	0.21	0.24	0.43	0.40	0.26	0.33	0.73	0.48
Kalalu (NRM)	0.09	0.36	0.55	0.21	0.40	0.52	0.61	0.75
Munyaka (NRM)	0.22	0.16	0.01	0.01	0.05	0.27	0.60	0.69
Lamu	0.27	0.54	0.73	0.71	0.49	0.85	0.82	0.63
Voi	0.29	0.48	0.10	0.67	0.57	0.70	0.89	0.68
Mombasa	0.15	0.63	0.57	0.67	0.19	0.28	0.57	0.62
Lodwar	0.38	0.58	0.35	0.35	0.20	0.32	0.72	0.21
Marsabit	0.18	0.01	0.64	0.29	0.51	0.88	0.81	0.25
Wajir	0.57	0.57	0.40	0.05	0.72	0.13	0.62	0.05
Narok	0.00	0.00	0.00	0.72	0.05	0.72	0.07	0.55
Mandera	0.16	0.18	0.67	0.02	0.53	0.47	0.82	0.36
Garissa	0.48	0.14	0.52	0.32	0.38	0.39	0.75	0.38
JKIA	0.19	0.15	0.11	0.55	0.22	0.79	0.66	0.65
Average	0.19	0.31	0.36	0.43	0.33	0.50	0.63	0.55

Legend:

▇	Maximum 0.90(+)
▢	Midpoint 0
▇	Minimum 0.90(-)

The amount of explained variability did not increase when grouping observations according to climatic zones. The highest R² (0.50) with a negative relationship between RUE and R95pTOT was observed during the short rains in semi-humid areas (Figure 9c) and semi-arid R² (0.40) (Figure 9b). The relation between R95pTOT index and RUE is moderate in semi-humid and semi-arid areas, where the correlation with CDD is weak (Table 8).

Table 8. R² representing the relationship between ANPP to extreme indices per location for both seasons long and short rains

Location	CDD		SDII		R95p%		R95pTOT	
	LR	SR	LR	SR	LR	SR	LR	SR
Arid	0.35	0.00	0.11	0.03	0.04	0.02	0.32	0.03
Semi-arid	0.01	0.06	0.01	0.32	0.00	0.14	0.01	0.40
Semi-humid	0.04	0.35	0.25	0.10	0.12	0.28	0.28	0.50
All station combined	0.00	0.05	0.00	0.02	0.00	0.00	0.02	0.02

Legend:

▇▇▇▇ ▢▢▢ ▇▇▇▇

Maximum 0.90(+)   Midpoint 0   Minimum 0.90(-)
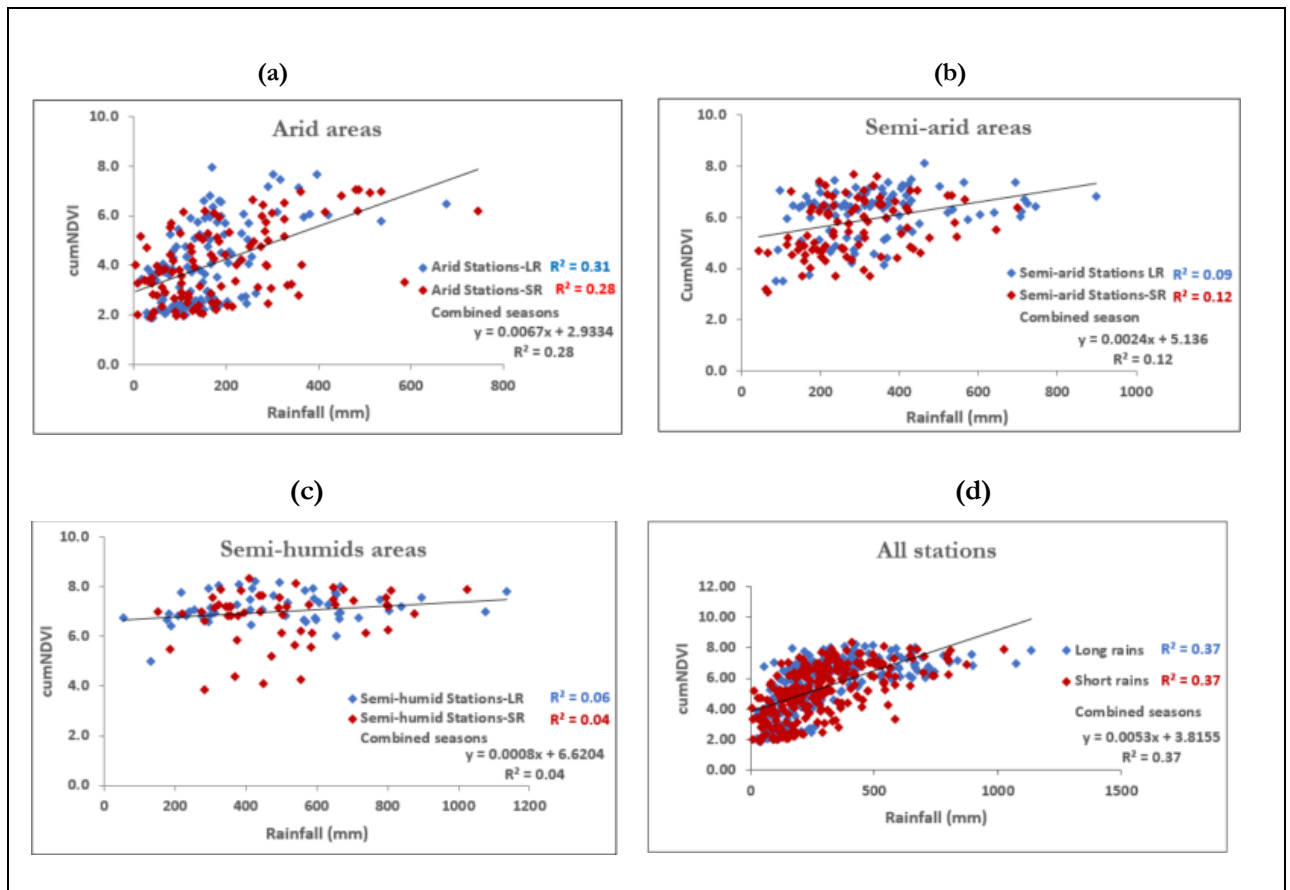
Figure 9. Scatterplots showing the relationship between RUE and R95pTOT for stations grouped; (a) arid areas, (b) semi-arid areas and (c) semi-humid areas

Figure 10 is showing the natural log transformation of the result done (Section 3.3.1) on the relation between RUE and extreme index for the three groups arid, semi-arid and semi-humid areas to improve the non-linear relationship observed between RUE and R95pTOT (Figure 9). The changes from this analysis are shown to be marginal compared to the result shown in Table 8 and Figure 9 with less improvement in some indices (Appendix III).
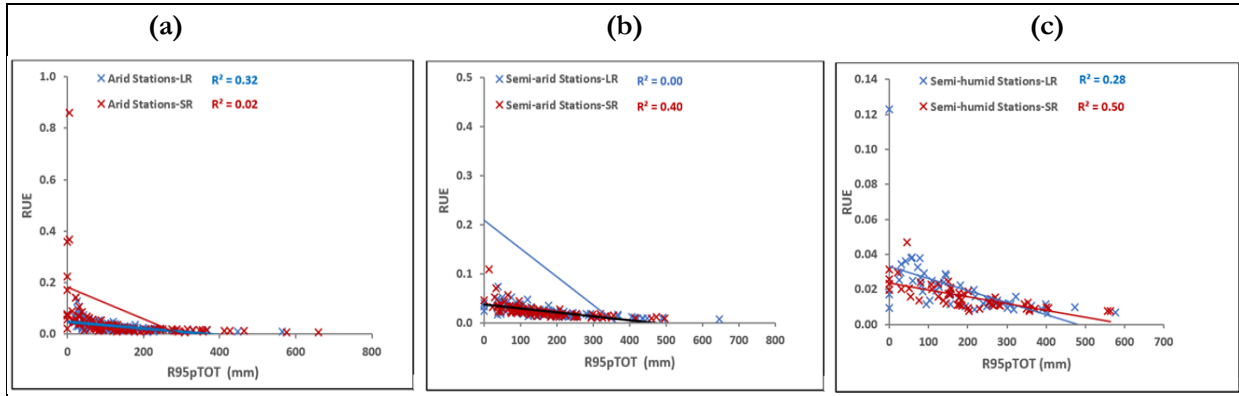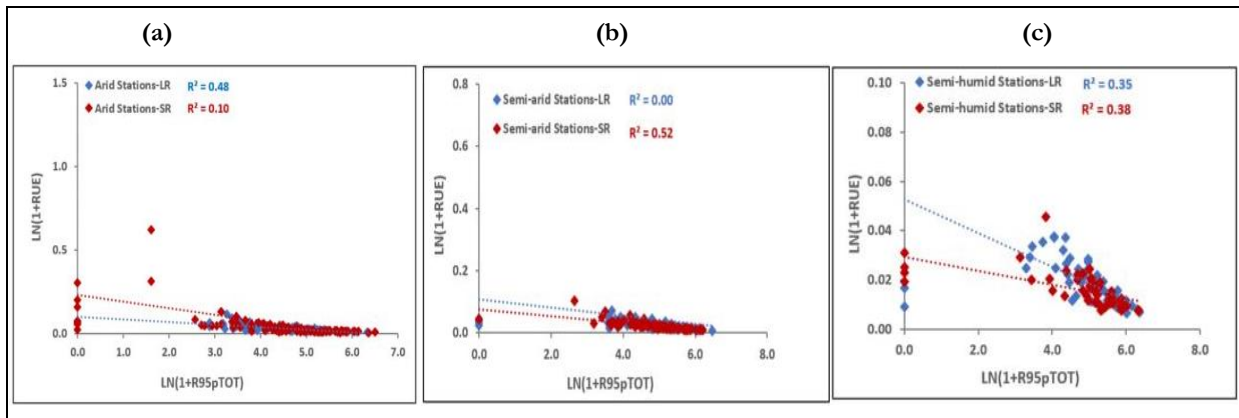

Figure 10. Scatterplots showing log-transformed relationship between RUE and R95pTOT for stations grouped (a) Arid areas, (b) Semi-arid areas and (c) Semi-humid areas

5.   DISCUSSION

This study found that extreme indices in within-season rainfall distribution explained a large fraction of the interannual RUE variability for most of the analyzed rainfall stations. It was also observed that within-seasonal rainfall distribution, as captured by extreme indices, could explain more than 60% of the interannual variability in RUE for most stations compared to total seasonal rainfall which could explain less than 50% of the interannual variability in vegetation productivity. The amount of variability that could be explained differed between station. Vegetation productivity is influenced by temporal patterns of precipitation distribution depends much on location (Yan et al., 2015). Because precipitation distribution is predicted to change to more extreme patterns with longer dry intervals and heavy rainfall (Zhang et al., 2013), the results presented in this thesis highlight that such changes may have important impacts on vegetation production in future climates.

This study shows that extreme precipitation patterns had lower RUE for most stations (Table 7). This explains that years with less frequent but more extreme distribution of precipitation had lower RUE for most stations related to years with less extreme precipitation. The decrease in productivity or RUE in these areas caused by the inability of plants to efficiently use rainfall in the season with more extreme distribution (Zhang et al., 2013). Huxman et al. (2004) also showed that plants respond effective to water inputs at moderate rainfall pattern and less effective to large heavy rainfall which leads to lower RUE. When rainfall pattern is more extreme cause less infiltration of water into the soil, hence runoff increases and cause water deficits (Arora et al., 2001).

The changes in seasonal rainfall distribution often cause water stress and a decrease in biomass. The impact of changes in seasonal rainfall distribution on vegetation production depends on the direction of the change in precipitation which also differs between seasons and location. Even when total seasonal rainfall may not change, the changes in seasonal precipitation may likely alter the relations between water and productivity. The result from this study was compared well with that of Zeppel et al. (2014) who showed that the effect of changing within-season distribution depends on location. Their study showed that at water-limited areas (xeri site) extreme precipitation increased soil water content and ANPP while at water-abundant (mesic site) it decreased soil water content and ANPP. For this study apart from individual station results (Table 7), also for grouped stations more extreme distribution have been observed to decreased vegetation productivity in water-limited areas and increase in some areas with less water stress (Figure 10). The difference in response highlights the importance of large heavy rainfall and longer dry periods interval within-seasonal rainfall distribution. The decrease in vegetation productivity with heavy precipitation without changing in total seasonal rainfall has been caused by increased water deficit in these areas. It is possible that the seasonal rainfall distribution had both more extreme precipitation and longer dry interval.

The length of dry spells within-seasonal rainfall distribution may cause an increase of more extreme water stress or decrease depending on the ecosystem. Knapp et al. (2008) have shown that though xeric ecosystem experience dry spells between rainfall, yet precipitation regime with few but heavy rainfall will increase soil water content. At mesic ecosystem may expose to more occurance of long dry periods which cause plant and soil water stress. The results of this study have shown that more extreme precipitation was attached with longer dry spells which caused plant and soil water limited. This means the decrease in productivity in most of the dry stations has been due to the several drought conditions in Kenya. The dry interval within-seasonal rainfall distribution in this study has been observed to be longer between season and season compared to that of Heisler-White et al. (2009) who had only the interval of 10-30 days. The result of their study leads to lower drought stress. This implies that the occurrence of longer dry spells and more extreme

precipitation in this study caused water stress conditions in the dry areas compares to wet areas, hence lead to reduce vegetation productivity.

In general, the response of more extreme precipitation without changing in total seasonal rainfall had shown a negative impact on RUE. The result of this study is supported by that of Ross et al. (2014) and Zhang et al. (2013), their studies found that more extreme precipitation with fewer but heavy rainfall patterns had strong negative impacts on vegetation productivity. Though in some areas vegetation productivity is increased as mean annual rainfall increase, the increase has been balanced by extreme precipitation. This means that mean annual rainfall is a useful climatic variable for predicting the response of vegetation to future climate change (Huxman et al., 2004; Knapp & Smith, 2001), where within-seasonal rainfall distribution can predict the response of some variability (Knapp et al., 2002).

Availability and quality of historical rainfall data is a key limitation for studying the effects of more extreme precipitation distribution on vegetation productivity. The principal restriction to scale this study to more site was the sparse distribution of rain gauges (Dinku et al., 2011), and the difficulty of accessing long-term archives of daily data even if they exist (Omondi et al., 2014). Due to data limitations, this study was not able to include more sites for a large area, which could have helped to better quantify differential effects of more extreme precipitation distribution on other biomes. However, extreme indices are calculated from a historical rain gauge with a length of 30-years climatological references period (Section 3.3). This study used a long-term rainfall data of only 16 years to extract extreme indices from the 19 rainfall stations across Kenya. Satellite-derived estimate of rainfall data (e.g. CHIRPS) could be used for this study since the daily product exist. The satellite product is based on estimate rainfall data which normally have inaccuracies, particularly for daily rainfall data. Rain gauge data are more accurate based on true ground measurement though they might not be inconsistency in data quality over time for a single station. Also, they have a longer available climatology data compared to satellite rainfall data. Therefore, for this study, the satellite products could not be accurate for describing the interannual variability of extreme indices because of over or underestimation of the amount of rainfall and frequency of extreme distribution (Dinku et al., 2011).

Some small error and uncertainties in the results of this study may occur because of input data used to estimate SOS_N and EOS_N dates. This is because the exact observation date for each NDVI observation was unknown for the eMODIS product, as used by Meroni et al. (2014) and Vrieling et al. (2016). Therefore, the central date for each 10-day composite was used. It can be expected this results on average in slightly earlier green-up dates and slightly later senescence dates (Vrieling et al., 2016).

Despite obtained estimate SOS_R and EOS_R dates for rainfall, some error of one to two months have occurred which caused a gap between the SOS_R /EOS_R and SOS_N/EOS_N dates. This lag period was also confirmed by other studies done in Kenya by Indeje et al. (2006) and Davenport & Nicholson (1993). The error may occur by using the 10-day cumulative rainfall data. This is because cumulating rainfall over the defined period tends to disregard the erratic day to day changes in rainfall that may influence on vegetation.

For further studies, it is important to examine the potential of improving the historical rain gauge data in East Africa and not only Kenya. This will help to validate this study by including other locations and biomes to understand the impacts of within-seasonal rainfall distribution on vegetation productivity. However, the results of this study reveal that season rainfall distribution, as captured by extreme precipitation indices, can also improve the prediction of seasonal vegetation productivity as compared to total seasonal rainfall.

6.   CONCLUSION

This study reveals the importance of within-season rainfall distribution in explaining the interannual variability of vegetation productivity. This has important implications for understanding and improving knowledge on the response of vegetation to extreme precipitation distribution under future climate change. Climate change has been causing changes in seasonal rainfall distribution with increasing in higher frequency of extreme precipitation distribution and longer dry periods. The results from this study showed how extreme precipitation distribution and not only total seasonal rainfall could improve prediction of vegetation productivity across biomes. The response of vegetation production to extreme precipitation has been observed being location dependent and changes in seasonal rainfall distribution. This study showed that the changes in seasonal precipitation frequently result in water stress in dry areas and reduced biomass compared to some wet areas. More extreme precipitation had shown negative impacts on vegetation production across biomes. The results suggest that under future climate change in the within-seasonal distribution of precipitation as more extreme precipitation and longer dry periods increase even when total seasonal rainfall remains unchanged, will likely reduce vegetation production in dry areas of Kenya. Furthermore, this study highlights the importance of accounting the interannual variability of rainfall in climatic models for the future climate change.

LIST OF REFERENCES

Allan, R. P., & Soden, B. J. (2008). Atmospheric warming and the amplification of precipitation extremes. *Science (New York, N.Y.)*, *321*(5895), 1481–4. https://doi.org/10.1126/science.1160787

Alterra, VITO, Consult, M., GISAT, & TAMSAT. (2013). *General Technical Description of data deliveries. Concept Version. Operational Activities for MARS Action-Period 3.ITT No. G03/06/07, LOT III.*

Arora, V. K., Chiew, F. H. S., & Grayson, R. B. (2001). Effect of sub-grid-scale variability of soil moisture and precipitation intensity on surface runoff and streamflow. *Journal of Geophysical Research-Atmospheres*, *106*(D15), 17073–17091. https://doi.org/10.1029/2001jd900037

CETRAD. (n.d.). Social and Hydrological Information Platform. Retrieved October 2, 2017, from http://wlrc-ken.org/data/timeseries/stations/1

Cumiskey, L., & Jackson, W. (2016). *Local level Preparedness and Response to the El Niño Phenomenon Early Warning in Tigithi, Kenya. Field Research Report.* Nairobi, Kenya. Retrieved from http://www.wateryouthnetwork.org/wp-content/uploads/2017/05/KENYA-EL-NINO-FINAL-REPORT-1.pdf

Davenport, M. L., & Nicholson, S. E. (1993). On the relation between rainfall and the Normalized Difference Vegetation Index for diverse vegetation types in East Africa. *International Journal of Remote Sensing*, *14*(12), 2369–2389. https://doi.org/10.1080/01431169308954042

de Beurs, K. M., & Henebry, G. M. (2010). Spatio-Temporal Statistical Methods for Modelling Land Surface Phenology. In *Phenological Research* (pp. 177–208). Dordrecht: Springer Netherlands. https://doi.org/10.1007/978-90-481-3335-2_9

Dinku, T., Ceccato, P., & Connor, S. J. (2011). Challenges of satellite rainfall estimation over mountainous and arid parts of east Africa. *International Journal of Remote Sensing*, *32*(21), 5965–5979. https://doi.org/10.1080/01431161.2010.499381

Dr.Kirubi, D., & Dr.Kahuthia-Gathu, R. (2012). KCU 201: PRINCIPLES OF CROP PRODUCTION. Retrieved January 9, 2018, from https://www.coursehero.com/file/p7bm808/Table-1-Moisture-availability-zones-in-Kenya-with-rainfall-and-proportion-of/

Dunning, C. M., Black, E. C. L., & Allan, R. P. (2016). The onset and cessation of seasonal rainfall over Africa. *Journal of Geophysical Research*, *121*(19), 11405–11424. https://doi.org/10.1002/2016JD025428

Easterling, D. R., Meehl, G. a, Parmesan, C., Changnon, S. a, Karl, T. R., & Mearns, L. O. (2000). Climate extremes: observations, modeling, and impacts. *Science's Compass*, *289*(5487), 2068–2074. https://doi.org/10.1126/science.289.5487.2068

ECA&D. (2017). Indices dictionary. Retrieved August 25, 2017, from http://eca.knmi.nl/indicesextremes/indicesdictionary.php

Fay, P. A., Kaufman, D. M., Nippert, J. B., Carlisle, J. D., & Harper, C. W. (2008). Changes in grassland ecosystem function due to extreme rainfall events : Implications for responses to climate change. *Global Change Biology*, *14*, 1600–1608. https://doi.org/10.1111/j.1365-2486.2008.01605.x

Heisler-White, J. L., Blair, J. M., Kelly, E. F., Harmoney, K., & Knapp, A. K. (2009). Contingent productivity responses to more extreme rainfall regimes across a grassland biome. *Global Change Biology*, *15*, 2894–2904. https://doi.org/10.1111/j.1365-2486.2009.01961.x

Heisler-White, Knapp, A. K., & Kelly, E. F. (2008). Increasing precipitation event size increases

aboveground net primary productivity in a semi-arid grassland. *Oecologia*, *158*(1), 129–140. https://doi.org/10.1007/s00442-008-1116-9

Herrmann, S. M., & Mohr, K. I. (2011). A continental-scale classification of rainfall seasonality regimes in Africa based on gridded precipitation and land surface temperature products. *Journal of Applied Meteorology and Climatology*, *50*(12), 2504–2513. https://doi.org/10.1175/JAMC-D-11-024.1

Hoscilo, A., Balzter, H., Bartholomé, E., Boschetti, M., Brivio, P. A., Brink, A., … Pekel, J. F. (2015). A conceptual model for assessing rainfall and vegetation trends in sub-Saharan Africa from satellite data. *International Journal of Climatology*, *35*(12), 3582–3592. https://doi.org/10.1002/joc.4231

Huntington, T. G. (2006). Evidence for intensification of the global water cycle: Review and synthesis. *Journal of Hydrology*, *319*, 83–95. https://doi.org/10.1016/j.jhydrol.2005.07.003

Huxman, T. E., Smith, M. D., Fay, P. A., Knapp, A. K., Shaw, M. R., Loik, M. E., … Williams, D. C. (2004). Convergence across biomes to common rain use efficiency. *Nature*, (April), 651–654. https://doi.org/10.1038/nature02597.1.

Huxman, T. E., Snyder, K. A., Tissue, D., Leffler, A. J., Ogle, K., Pockman, W. T., … Schwinning, S. (2004). Precipitation pulses and carbon fluxes in semiarid and arid ecosystems. *Oecologia*, *141*(2), 254–268. https://doi.org/10.1007/s00442-004-1682-4

Indeje, M., Ward, M. N., Ogallo, L. J., Davies, G., Dilley, M., & Anyamba, A. (2006). Predictability of the Normalized Difference Vegetation Index in Kenya and Potential Applications as an Indicator of Rift Valley Fever Outbreaks in the Greater Horn of Africa, *19*, 1673–1687. Retrieved from http://pordlabs.ucsd.edu/ltalley/sio219/indeje_etal_jclimate2006.pdf

IPCC. (2012). *Mnaging the Risks of Extreme Events and Disasters to Advance Climate Change Adaptation. A special report of Working Groups I and II of Intergovernmental Panel on Climate Change*. Cambridge, United Kingdom and New York, NY, USA. Retrieved from https://www.ipcc.ch/pdf/special-reports/srex/SREX_Full_Report.pdf

IPCC,2014:Climate Change 2014, Synthesis Report.Contribution of Working Groups I, II and III to the Fifth Assessment Report of the Intergovernmental Panel on Climate Change [Core Writing Team, R.K Pachauri and L.A Meyer (eds.)]. (2014). IPCC, Geneva, Switzerland. Retrieved from http://www.ipcc.ch/pdf/assessment-report/ar5/syr/SYR_AR5_FINAL_full_wcover.pdf

IPCC, 2014. (2014). *Africa. Cambridge University Press,*. Cambridge, United Kingdom and Mew York, NY, USA. Retrieved from https://www.ipcc.ch/pdf/assessment-report/ar5/wg2/WGIIAR5-Chap22_FINAL.pdf

Jenkerson, C. B., Scientist, S., & Schmidt, G. L. (2008). *eMODIS product access for large scale monitoring eMODIS rationale. SAIC, Contractor to U.S. Geological Survey*. Denver, Colorado.

Kabubo-Mariara, J., & Kabara, M. (2015). Climate Change and Food Security in Kenya. *Environment for Development*, 1–36. Retrieved from http://www.efdinitiative.org/sites/default/files/publications/efd-dp-15-05.pdf

Kang, Y., Khan, S., & Ma, X. (2009). Climate change impacts on crop yield , crop water productivity and food security – A review. *Progress in Natural Science*, *19*(12), 1665–1674. https://doi.org/10.1016/j.pnsc.2009.08.001

Kimani, S. K., Esilaba, A. O., Njeru, P. N. M., Miriti, J. M., Lekasi, J. K., & Koala, S. (2014). Situation Analysis of Climate Change Aspects in Kenya. In *Adapting African Agriculture to Climate Change* (pp. 43–52). Switzerland: Springer International Publishing. https://doi.org/10.1007/978-3-319-13000-2

Knapp, A. K., Beier, C., Briske, D. D., Classen, A. T., Luo, Y., Reichstein, M., … Weng, E. (2008).

Consequences of More Extreme Precipitation Regimes for Terrestrial Ecosystems. *BioScience*, *58*(9), 811. https://doi.org/10.1641/B580908

Knapp, A. K., Fay, P. ., Blair, J. ., Collins, S. ., Smith, M. ., Carlisle, J. ., … McCarron, J. . (2002). Rainfall Variability, Carbon Cycling, and Plant Species Diversity in a Mesic Grassland. *Science*, *298*(5601), 2202–2205. https://doi.org/10.1126/science.1076347

Knapp, A. K., & Smith, M. D. (2001). Variation Among Biomes in Temporal Dynamics of Aboveground Primary Production. *Science*, *291*(5503), 481–484. https://doi.org/10.1126/science.291.5503.481

Liebmann, B., Bladé, I., Kiladis, G. N., Carvalho, L. M. V, Senay, G. B., Allured, D., … Funk, C. (2012). Seasonality of African precipitation from 1996 to 2009. *Journal of Climate*, *25*(12), 4304–4322. https://doi.org/10.1175/JCLI-D-11-00157.1

Liebmann, B., & Marengo, J. A. (2001). Interannual variability of the rainy season and rainfall in the Brazilian Amazon Basin. *Journal of Climate*, *14*(22), 4308–4318. https://doi.org/10.1175/1520-0442(2001)014<4308:IVOTRS>2.0.CO;2

Lomb, N. R. (1976). LEAST-SQUARES FREQUENCY ANALYSIS OF UNEQUALLY SPACED DATA. *Astrophysics and Space Science*, *39*, 447–462. Retrieved from https://link.springer.com/content/pdf/10.1007%2FBF00648343.pdf

Meroni, M., Verstraete, M. M., Rembold, F., Urbano, F., & Kayitakire, F. (2014). A phenology-based method to derive biomass production anomalies for food security monitoring in the Horn of Africa. *International Journal of Remote Sensing*, *35*(7), 2472–2492. https://doi.org/10.1080/01431161.2014.883090

Muchemi, G. M., Thumbi, S. M., Kiama, S. G., & Nanyingi, M. O. (2012). Climate change vulnerability, adaptation and mitigation of livestock systems in Kenya.Wangari Maathai Institute for Environmental Studies and Peace, College of Agriculture and Veterinary Science, University of Nairobi, Nairobi,Kenya. Retrieved July 29, 2017, from http://erepository.uonbi.ac.ke/handle/11295/72433

Omondi, P. A., Awange, J. L., Forootan, E., Ogallo, L. A., Barakiza, R., Girmaw, G. B., … Komutunga, E. (2014). Changes in temperature and precipitation extremes over the Greater Horn of Africa region from 1961 to 2010. *International Journal of Climatology*, *34*(4), 1262–1277. https://doi.org/10.1002/joc.3763

Owiti, Z. (2012). Spatial distribution of rainfall seasonality over East Africa. *Journal of Geography and Regional Planning*, *5*(15), 409–421. https://doi.org/10.5897/JGRP12.027

Ross I. Maidment, David Grimes, Richard P. Allan, Elena Tarnavsky, Marc Stringer, Tim Hewison, Rob Roebeling, and E. B. (2014). Journal of Geophysical Research: Atmospheres And Time series (TARCAT) data set. *Journal of Geophysical Research: Atmospheres*, *119*, 10619–10644. https://doi.org/10.1002/2014JD021927.Received

Rufino, M. C., Thornton, P. K., Ng'ang'a, S. K., Mutie, I., Jones, P. G., van Wijk, M. T., & Herrero, M. (2013). Transitions in agro-pastoralist systems of East Africa: Impacts on food security and poverty. *Agriculture, Ecosystems and Environment*, *179*, 215–230. https://doi.org/10.1016/j.agee.2013.08.019

Scargle, J. D. (1982). Studies in astronomical time series analysis. II - Statistical aspects of spectral analysis of unevenly spaced data. *The Astrophysical Journal*, *263*, 835. https://doi.org/10.1086/160554

Swets, D. L., Reed, B. C., Rowland, J. D., & Marko, S. E. (1999). A Weighted Least-Squares Approach to Temporal NDVI Smoothing. Proceedings of the 1999 ASPRS Annual Conference, (Figure 1), (pp. 526–536). Retrieved from https://phenology.cr.usgs.gov/pubs/ASPRS Swets et al Smoothing.pdf

Tierney, J. E., Ummenhofer, C. C., & DeMenocal, P. B. (2015). Past and future rainfall in the Horn of Africa. *Science Advances*, *1*(9), e1500682–e1500682. https://doi.org/10.1126/sciadv.1500682

Uhe, P., Philip, S., Kew, S., Shah, K., Kimutai, J., Mwangi, E., … Otto, F. (2017). Attributing drivers of the 2016 Kenyan drought. *International Journal of Climatology*. https://doi.org/10.1002/joc.5389

VanderPlas, J. T. (2017). Understanding the Lomb-Scargle Periodogram, 1–55. Retrieved from http://arxiv.org/abs/1703.09824

Vrieling, A., Meroni, M., Mude, A. G., Chantarat, S., Ummenhofer, C. C., & de Bie, K. C. A. J. M. (2016). Early assessment of seasonal forage availability for mitigating the impact of drought on East African pastoralists. *Remote Sensing of Environment*, *174*, 44–55. https://doi.org/10.1016/j.rse.2015.12.003

Vrieling, A., Meroni, M., Shee, A., Mude, A. G., Woodard, J., de Bie, C. A. J. M., & Rembold, F. (2014). Historical extension of operational NDVI products for livestock insurance in Kenya. *International Journal of Applied Earth Observation and Geoinformation*, *28*, 238–251. https://doi.org/10.1016/j.jag.2013.12.010

Walsh, R. P. D., & Lawler, D. M. (1981). Rainfall seasonality: Description, Spatial patters and change trough time. *Weather*, *36*(7), 201–208. https://doi.org/10.1002/j.1477-8696.1981.tb05400.x

WMO. (2009). *Analysis of extremes in a changing climate in support of informed decision for adaptation*. Geneva 2, Switzerland. Retrieved from http://www.wmo.int

Yan, H., Liang, C., Li, Z., Liu, Z., Miao, B., He, C., & Sheng, L. (2015). Impact of precipitation patterns on biomass and species richness of annuals in a dry steppe. *PLoS ONE*, *10*(4), 1–14. https://doi.org/10.1371/journal.pone.0125300

Zeppel, M. J. B., Wilks, J. V., & Lewis, J. D. (2014). Impacts of extreme precipitation and seasonal changes in precipitation on plants. *Biogeosciences*, *11*(11), 3083–3093. https://doi.org/10.5194/bg-11-3083-2014

Zhang, Moran, M. S., Nearing, M. A., Campos, G. E. P., Huete, A. R., Buda, A. R., … Starks, P. J. (2013). Extreme precipitation patterns and reductions of terrestrial ecosystem production across biomes, *118*, 148–157. https://doi.org/10.1029/2012JG002136

APPENDICES

Appendix I.

Scatterplots showing the relationship between cumNDVI and total seasonal rainfall for all the stations.
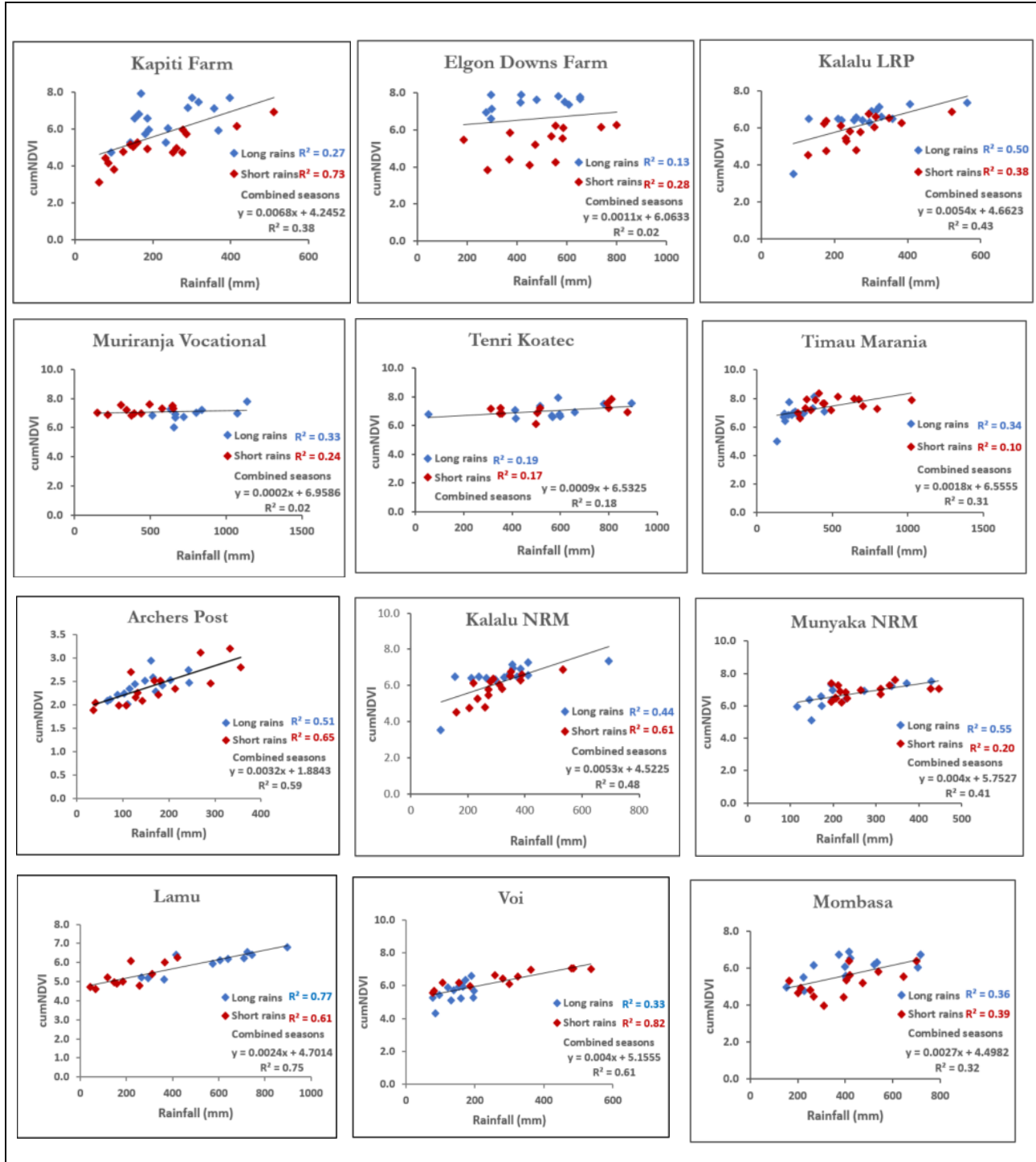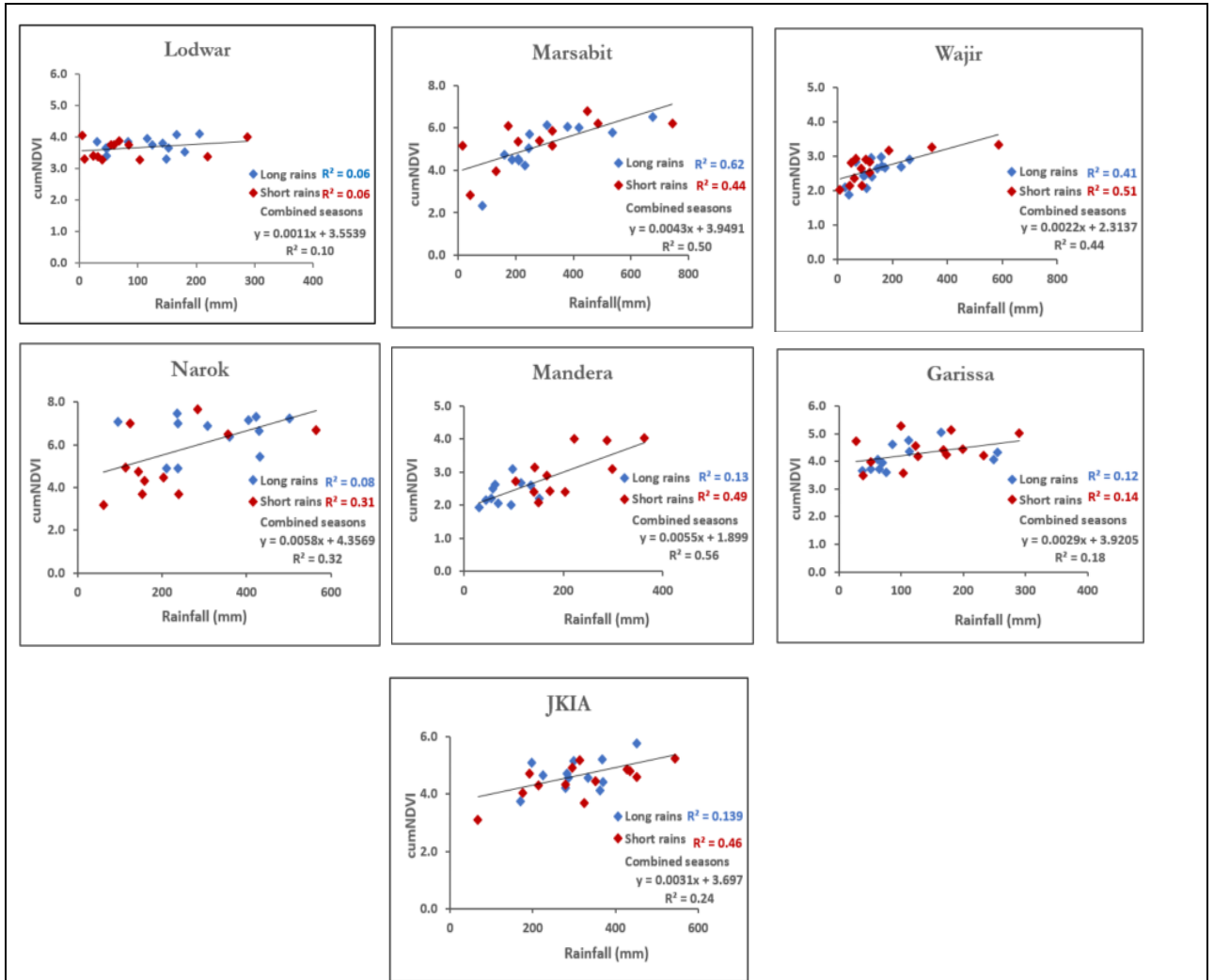
Appendix II.

ANOVA single factor summary tables showing the significant difference between climatic zone groups per season

SUMMARY

Groups	Count	Sum	Average	Variance
Arid areas-LR	8	0.7911885	0.0988986	0.0112375
Arid areas-SR	8	0.4516082	0.056451	0.0081175
Semi-arid areas-LR	7	0.593525	0.0847893	0.0186783
Semi-arid areas-SR	7	0.2054553	0.0293508	0.0012995
Semi-humid areas-LR	4	0.4245378	0.1061345	0.0050661
Semi-humid areas-SR	4	0.6143231	0.1535808	0.0058863

ANOVA

Source of Variation	SS	df	MS	F	P-value	F-critical
Between Groups	0.0497568	5	0.0099514	1.1049024	0.3771945	2.5122549
Within Groups	0.2882094	32	0.0090065			
Total	0.3379662	37				

Dependent Variable: Long Rains

Games-Howell

(I) Location	(J) Location	Mean Difference (I-J)	Std. Error	Sig.	95% Confidence Interval Lower Bound	Upper Bound
Arid	semi-arid	.01410927930	.063820228200	.973	-.15759233900	.18581089800
	semi-humid	-.00723589800	.051683877300	.989	-.15233745700	.13786566100
semi-arid	Arid	-.01410927930	.063820228200	.973	-.18581089800	.15759233900
	semi-humid	-.02134517730	.062728550000	.939	-.19650270400	.15381235000
semi-humid	Arid	.00723589800	.051683877300	.989	-.13786566100	.15233745700
	semi-arid	.02134517730	.062728550000	.939	-.15381235000	.19650270400

Dependent Variable: Short rains

Games-Howell

(I) Location	(J) Location	Mean Difference (I-J)	Std. Error	Sig.	95% Confidence Interval Lower Bound	Upper Bound
Arid	semi-arid	2.710026E-002	3.4645797E-002	.722	-6.882818E-002	1.230287E-001
	semi-humid	-9.712976E-002	4.9862459E-002	.195	-2.434066E-001	4.914710E-002
semi-arid	Arid	-2.710026E-002	3.4645797E-002	.722	-1.230287E-001	6.882818E-002
	semi-humid	-1.242300E-001	4.0708889E-002	.085	-2.734114E-001	2.495132E-002
semi-humid	Arid	9.712976E-002	4.9862459E-002	.195	-4.914710E-002	2.434066E-001
	semi-arid	1.242300E-001	4.0708889E-002	.085	-2.495132E-002	2.734114E-001

Appendix III.

Scatterplots showing the relationship between RUE and extreme index R95pTOT rainfall for all some stations.
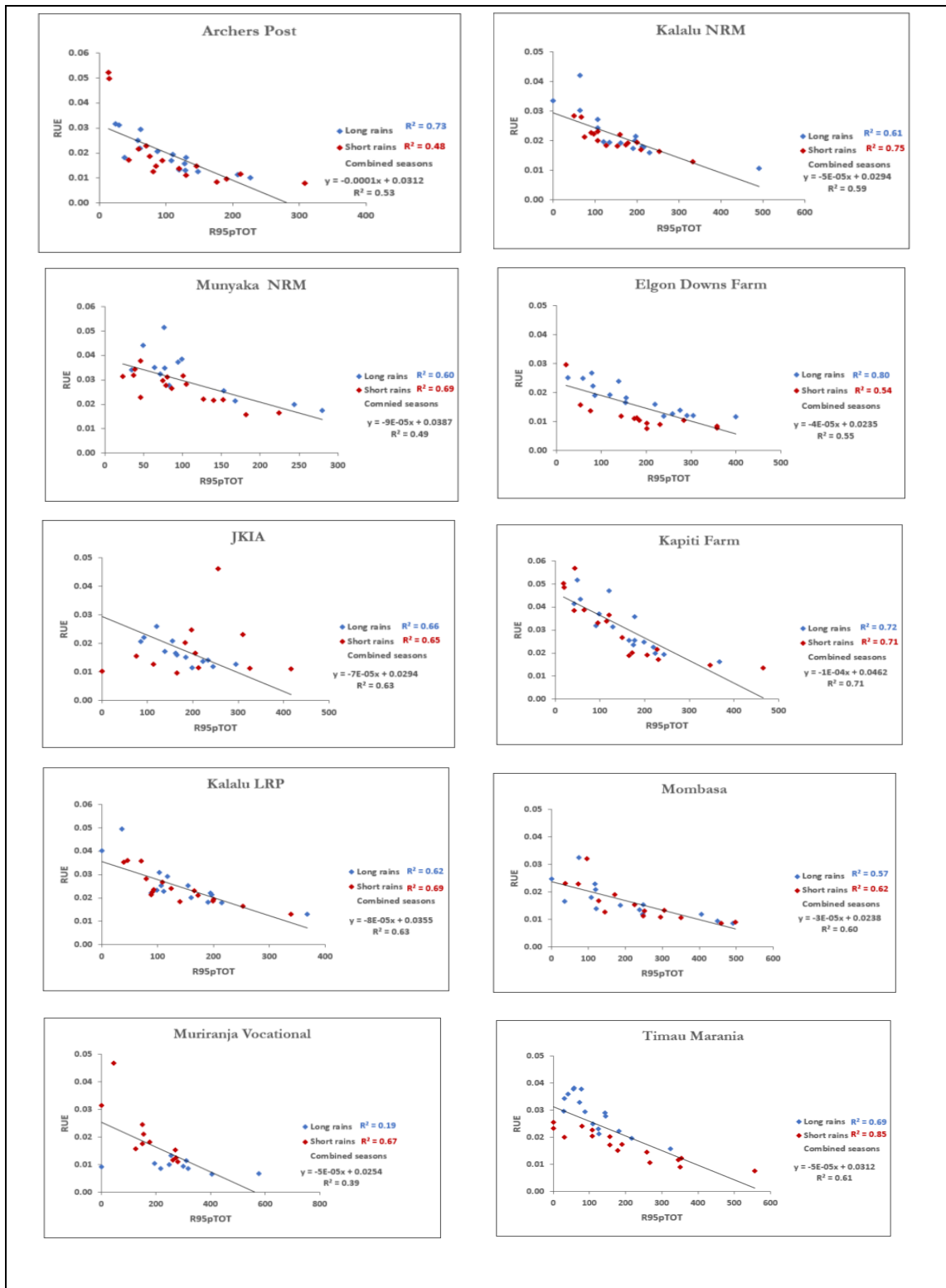
Appendix IV.

Table showing results of log-transformed regression for the relationship between RUE and R95pTOT for stations grouped per climatic zones

Grouped station								
	LN(1+CDD)		LN(1+SDII)		LN(1+R95p%)		LN(1+R95pTOT)	
Location	LR	SR	LR	SR	LR	SR	LR	SR
Arid	0.10	0.01	0.17	0.07	0.05	0.03	0.51	0.10
Semi-arid	0.00	0.11	0.11	0.43	0.00	0.15	0.00	0.52
Semi-humid	0.11	0.14	0.28	0.06	0.13	0.29	0.35	0.38
All station combined	0.00	0.01	0.00	0.05	0.00	0.00	0.00	0.08